Available online at www.sciencedirect.com
ScienceDirect
Trans. Nonferrous Met. Soc. China 19(2009) 341−346
Transactions of Nonferrous Metals Society of China
www.tnmsc.cn

Sensing controlled pulse key-holing condition in plasma arc welding

JIA Chuan-bao(贾传宝)[1], WU Chuan-song(武传松)[1], ZHANG Yu-ming(张裕明)[2]

1. Institute for Materials Joining, Shandong University, Jinan 250061, China;
2. Center for Manufacturing, University of Kentucky, Lexington, KY 40506, USA

Received 25 April 2008; accepted 25 August 2008

Abstract: According to the strategy of controlled pulse key-holing, a new sensing and control system was developed for monitoring and controlling the keyhole condition during plasma arc welding (PAW). Through sensing and processing the efflux plasma voltage signals, the quantitative relationship among the welding current, efflux plasma voltage and backside weld width of the weld was established. PAW experiments show that the efflux plasma voltage can reflect the state of keyhole and backside weld width accurately. The closed-loop control tests validate the stability and reliability of the developed keyhole PAW system.

Key words: controlled pulse key-holing; efflux plasma voltage; keyhole; plasma arc welding

1 Introduction

High-performance metals like aluminum alloy and stainless steel should be welded by high energy density welding technologies such as plasma arc welding(PAW), laser beam welding(LBM) and electron beam welding (EBW). Compared with LBW and EBW, PAW is a process with low cost and easy operation[1−3]. During PAW process, keyhole is formed inside the weld pool, and it is sensitive to any changes of the welding parameters. Whether the keyhole condition is in quasi-steady state or not critically determines the stability of welding process and the quality of weld joints [4]. To expand the parameters window for quasi-steady keyhole condition, pulsed current PAW is invented to produce one keyhole for each pulse. But this technique is just applicable for welding thinner plates[5]. To weld thicker materials, a new strategy termed as controlled pulse key-holing was proposed, and an experimental system was developed[6]. However, the key issue is how to sense and monitor the condition of controlled pulse key-holing, and further to realize the closed-loop control of PAW process with this new strategy.

Various kinds of methods have been used to monitor the keyhole condition, such as efflux plasma voltage sensors, optical sensors, sound signal sensors and plasma cloud charge sensors. Once the feedback signals of keyhole condition are acquired, the welding process parameters can be adjusted synchronously to control the stability of the keyhole[7−14]. But the sensing methods mentioned above have some limitations, for example, optical sensors need long time to transfer signals and cost a lot, and sound signal sensors are not accurate enough. The efflux plasma voltage sensor, which measures the electrical potential between the workpiece and the detection plate when the keyhole is established and the plasma jet exits through the keyhole, is employed to sense the keyhole condition and control the PAW process [15−17]. Such efflux plasma voltage sensor has some disadvantages, i.e., the detection plate has to be mounted on the backside of the workpiece, but its cost is low, its structure is simple, and its reliability is high.

In this study, the controlled pulse key-holing strategy was combined with the efflux plasma voltage sensor to realize the closed-loop control of keyhole PAW process.

2 System structure and sensing technique

As shown in Fig.1, the developed PAW welding system consisted of the computer, PAW machine, data acquisition card, efflux plasma voltage sensor and current sensor etc. The computer was the central unit of

Foundation item: Project(50540420570) supported by the National Natural Science Foundation of China; Project(07-12-002) supported by the Innovative Conception Fund of the Welding Institution of Chinese Mechanical Engineering Society
Corresponding author: WU Chuan-song; Tel: +86-531-88392711; E-mail: wucs@sdu.edu.cn
DOI: 10.1016/S1003-6326(08)60275-7

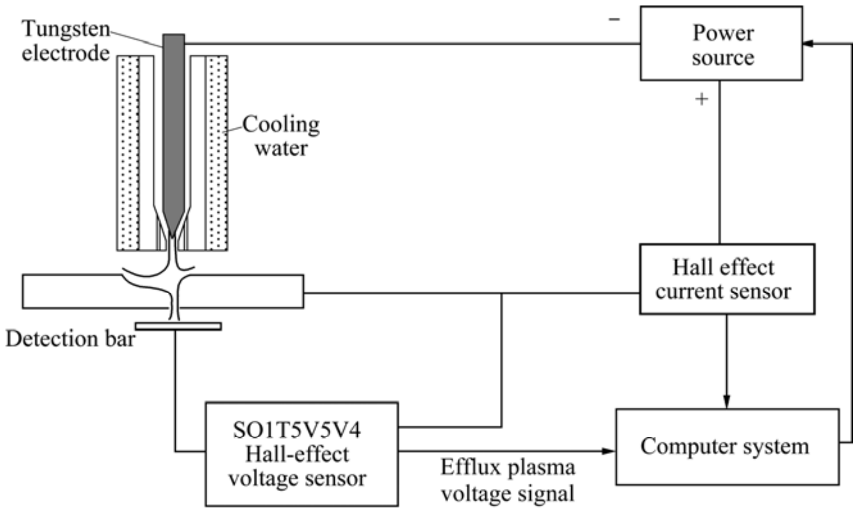

Fig.1 Schematic of experimental system

the system. On one hand, it could adjust welding current in real time and output any current waveforms as user-defined[6]. On the other hand, it sampled the signals of welding current and efflux plasma voltage. A piece of mild-steel sheet was chosen as the detection bar mounted underneath the workpiece to be welded and kept insulated. The distance between the workpiece and the detection bar was fixed at about 6 mm.

When the workpiece was completely penetrated and a keyhole was established, the efflux plasma exited through the keyhole. Due to the phenomenon of plasma space charge, the efflux plasma established an electrical potential between the workpiece and the detection bar, which was isolated from the workpiece. However, if the keyhole was not established or closed because of insufficient heat and force actions, there was no efflux plasma between the workpiece and the detection bar and thus no electrical potential was established. Hence, the electrical potential could be measured to determine the intensity of the efflux plasma, and thus to establish the keyhole. As shown in Fig.1, an integrated Hall-effect element SO1T5V5V4 connected between the detection bar and the workpiece was used to measure the electrical potential resulted from the efflux plasma. The sensing element could quickly response to the variation of efflux plasma voltage and could insulate the computer system to prevent the interferences from the welding process. Its output was sampled by the data acquisition card inserted inside the computer without extra resistance-capacitance (RC) circuit as shown in Refs.[15−17].

3 Sensing experiments

Welding experiments under open-loop control condition were conducted. The welding current and efflux plasma voltage were measured in real time to observe the changes of efflux plasma voltage when keyhole was established during the keyhole PAW process. The welding conditions were as follows. The welded material was stainless steel 1Cr18Ni9Ti, the workpiece thickness was 6 mm, the distance from the nozzle to the workpiece was 6 mm, the shielding gas and the plasma gas were Argon, and the flow rates were 20.0 L/min and 3.0 L/min, respectively, and the welding speed was 120 mm/min.

The experimental results are shown in Fig.2. At the starting segment of weld (about 22 mm in length), the workpiece was not fully penetrated under the conditions mentioned above. Because no keyhole was established, there was no efflux plasma, and the acquired efflux plasma voltage signal was close to zero. As the welding process continued, the thermal condition on the workpiece was improved, and the workpiece was fully penetrated at about 13 s after plasma arc was ignited. Then keyhole was established, the efflux plasma exited and the efflux plasma voltage(V_E) increased from 0 to about 1.2 V. When the welding process ended, the welding current was decreased to zero, the keyhole was closed, and the efflux plasma voltage(V_E) returned to zero. It could be seen that the amplitude of acquired efflux plasma voltage signals could be used to reflect the condition whether the keyhole was formed or not.

In order to further study the relationship of welding current, efflux plasma voltage and backside weld width, experiments were conducted using various levels of welding current. Other welding conditions were as the same as those mentioned above. After welding, the welded workpieces were sectioned, and the macro-photographs of cross-section welds as shown in Fig.3 were obtained. Through observing these macro-photographs, the penetration extent and the weld width

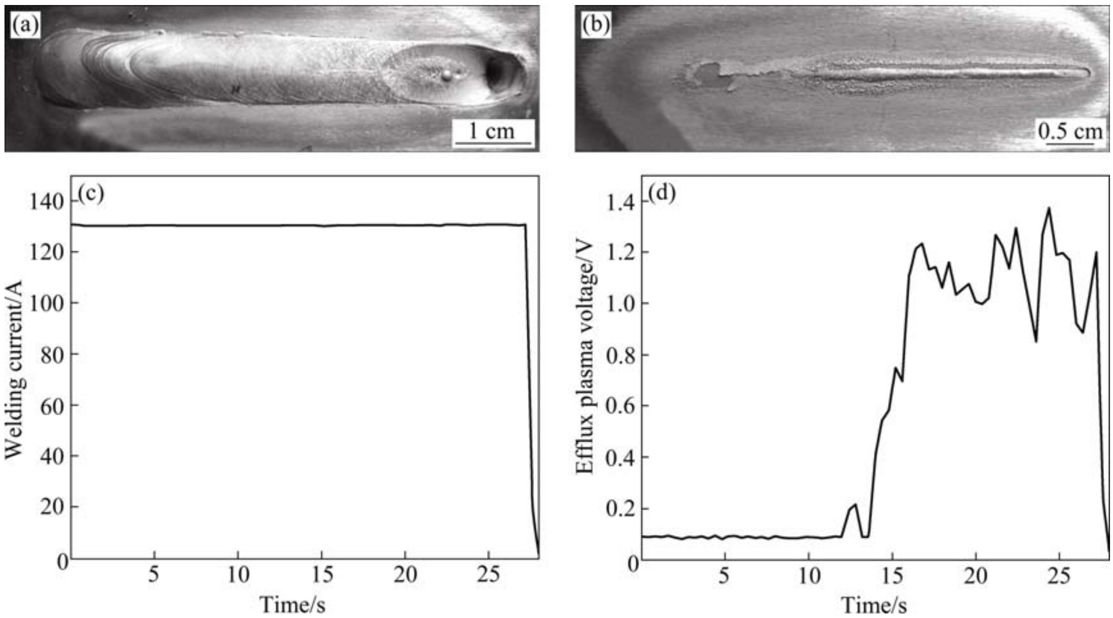

Fig.2 Experimental results: (a) Topside weld; (b) Backside weld; (c) Welding current signal; (d) Efflux plasma voltage signal

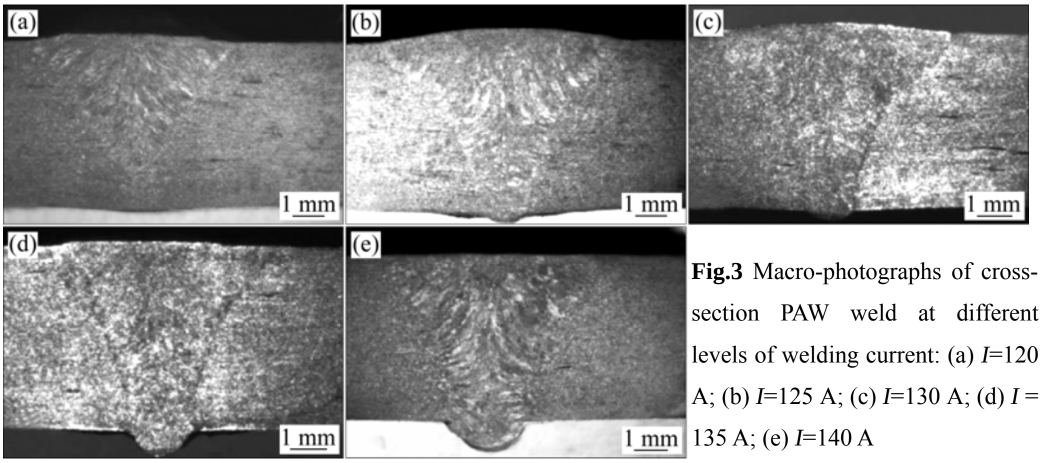

Fig.3 Macro-photographs of cross-section PAW weld at different levels of welding current: (a) I=120 A; (b) I=125 A; (c) I=130 A; (d) I = 135 A; (e) I=140 A

on backside can be known. During the welding processes at different levels of welding current, the efflux plasma voltage signals were measured and recorded (Fig.4). The symbols of I, W_B and V_E are used to represent the welding current, backside weld width and efflux plasma voltage, respectively.

As shown in Fig.3(a) and Fig.4(a), when I=120 A, the workpiece was not penetrated (W_B=0 mm), and no efflux plasma voltage signals were acquired (V_E=0). When I=125 A, the workpiece was penetrated through but with small backside width (W_B=1.12 mm) in Fig.3(b), and a low amplitude of the efflux plasma voltage signals was acquired (V_E=1.2 V) in Fig.4(b). As the welding current increased, the keyhole became bigger. When the current were 130, 135 and 140 A, W_B was measured as 1.54, 1.97 and 2.69 mm, as shown in Figs.3(c), (d) and (e) respectively and V_E in stable condition was estimated as 1.8, 2.5 and 3.0 V correspondingly, as shown in Figs.4(c), (d), and (e). The correlations of I, W_B and V_E are illustrated in Fig.5. It can be seen that there is a strong dependence of both W_B and V_E on current I. During the PAW processes, increasing of welding current within some ranges caused stronger heat and force action from the arc plasma, so that the keyhole dimension grows with the increase in welding current. The growing of keyhole dimension resulted in increasing of efflux plasma voltage. As shown in Fig.5, both the efflux plasma and the backside weld width are proportional to the welding current, and there is a linear relationship between the backside weld width(W_B) and the efflux plasma voltage (V_E). Therefore, the measured value of V_E can describe the key-holing condition in the PAW process.

4 Controlling experiments

Fig.6 shows the welding current waveform employed in the strategy of controlled pulse key-holing. For any welding condition, a peak current value large

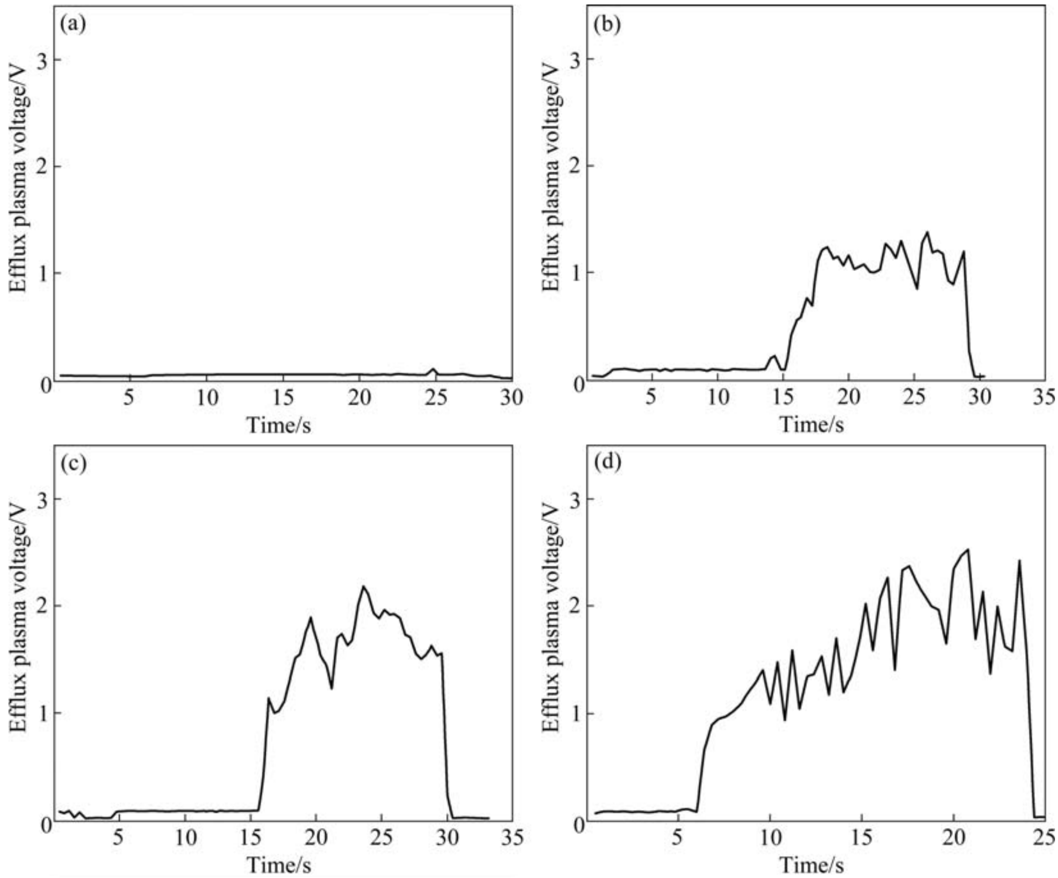

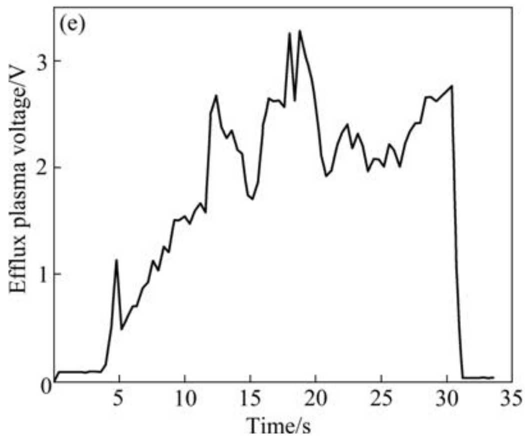

Fig.4 Efflux plasma voltage signals at different levels of welding current: (a) I=120 A; (b) I =125 A; (c) I=130 A; (d) I=135 A; (e) I=140 A

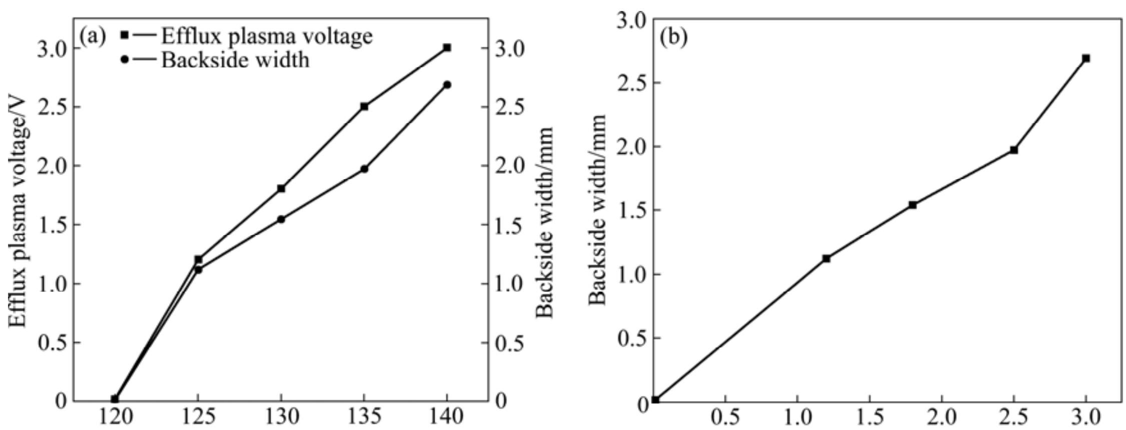

Fig.5 Correlations of welding current(I), efflux plasma voltage(V_E) and backside width(W_B): (a) Relationship of V_E, W_B and I; (b) Relationship between V_E and W_B

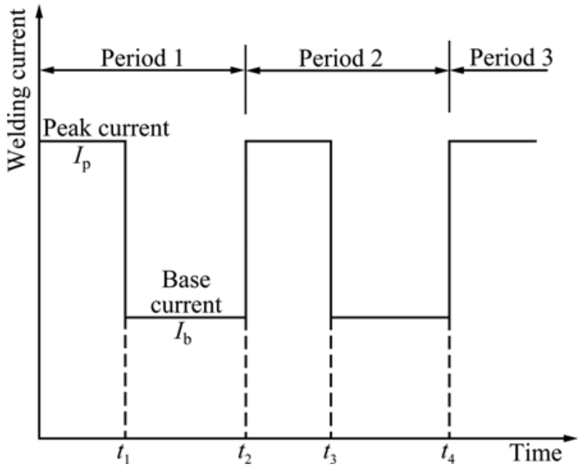

Fig.6 Schematic of welding current waveform

enough should first be applied to assure the penetration and formation of keyhole. Once keyhole forms and reaches a certain size, the welding current will be lowered to base value immediately to make the keyhole close. When the keyhole closes, the current is increased to peak value again and the whole process is repeated. This strategy can assure that the workpiece is fully penetrated and over-penetration and burn-through are avoided at the same time.

To validate the system and the control strategy, controlled pulse key-holing welding experiments were conducted. The welding conditions were as follows: peak current I_P=160 A, and base current I_B=80 A. Other welding conditions were as the same as the experiments mentioned above. The experimental results are shown in Fig.7. Figs.7(a) and (b) show parts of the acquired welding current and corresponding efflux plasma voltage signals, respectively. Both sampled signals were in quasi-steady state. The efflux plasma voltage(V_E) fluctuated between 0 and 2.8 V with the mean value around 1.0 V. While the welding current changed between the peak and base levels, the efflux plasma voltage(V_E) varied from its peak to its base value, thus the keyhole was open and closed correspondingly. Due to the fact that the system required certain time to response to the variation of key-holing condition, the welding current and efflux plasma signals were not in strict synchronization, which made the pulse and base current duration and base level change within some ranges so that the process parameters window was widened to some extent.

Figs.7(c) and (d) show the macro-photographs of cross-section weld and the backside weld appearance. It can be seen that full penetration and good quality of weld are ensured during the controlled pulse key-holing PAW process.

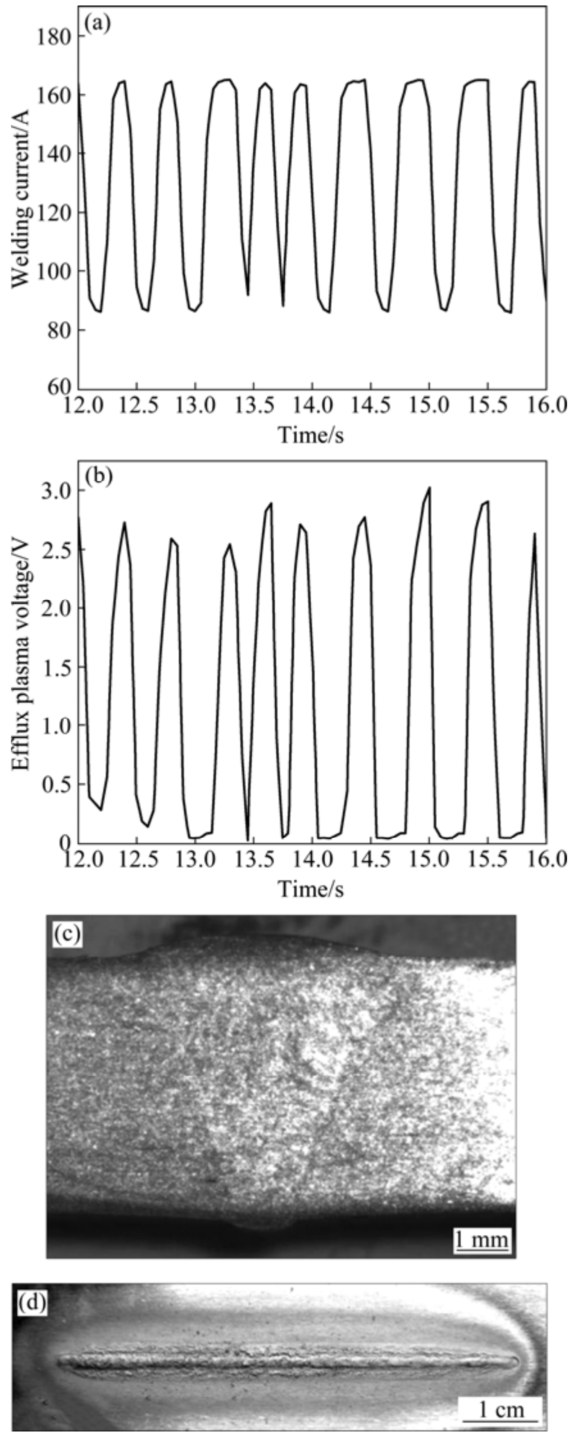

Fig.7 PAW control experiment results (I_P=160 A, I_B=80 A): (a) Welding current (12−16 s); (b) Efflux plasma voltage (12−16 s); (c) Macro-photograph of cross-section weld; (d)Backside weld appearance

5 Conclusions

1) Based on the strategy of controlled pulse key-holing, a sensing and control system for plasma arc welding is developed. Through measuring the efflux plasma voltage with a detection bar, the keyhole

condition can be determined.

2) The linear relationship among the welding current, efflux plasma voltage and backside weld width exists so that the efflux plasma voltage signals can be used to control the penetration extent of PAW process.

3) Through employing the controlled pulse key-holing strategy, keyhole PAW process control is realized. And the PAW process is stable and satisfactory weld formation is obtained.

References

[1] METCALFE J C, QUIGLEY M B C. Heat transfer in plasma-arc welding [J]. Welding Journal, 1975, 54(3): 99−103.

[2] LANCASTER J F. The physics of welding [M]. 15th ed. Oxford: Pergamon Press, 1984: 268−280.

[3] WU Chuan-song, WANG Huai-gang, ZHANG Yu-ming. A new heat source model for keyhole plasma arc welding in FEM analysis of the temperature profile [J]. Welding Journal, 2006, 85(12): 284−291.

[4] DONG Chun-lin, WU lin, SHAO Yi-chen. The history and state-of-the-art of keyhole mode plasma arc welding [J]. China Mechanical Engineering, 2000, 11(5): 577−581. (in Chinese)

[5] ZHU Yi-feng, ZHANG Hui, SHAO Yi-chen, DONG Chun-lin. Pulse plasma arc welding technology [J]. Aeronautical Manufacturing Technology, 1999, S1: 53−54.

[6] JIA Chuan-bao, WU Chuan-song, ZHANG Yu-ming. A computer-based control system for keyhole plasma arc welding [J]. China Welding, 2007, 16(1): 7−10. (in Chinese)

[7] ZHANG Y M, LIU Y C. Control of dynamic keyhole welding process [J]. Automatica, 2007, 43: 876−884.

[8] ZHANG Y M, ZHANG S B, LIU Y C. A plasma cloud charge sensor for pulse keyhole process control [J]. Measurement Science and Technology, 2001, 12(8): 1365−1370.

[9] WANG Yao-wen, CHEN Qiang, SUN Zhen-guo, SUN Jiu-wen, WANG Hai-yan. Sound sensing of the keyhole behaviors in plasma arc welding [J]. Chinese Journal of Mechanical Engineering, 2001, 37(1): 53−56. (in Chinese)

[10] CHEN Qiang, SUN Zhen-guo, SUN Jiu-wen, WANG Yao-wen. Closed-loop control of welding penetration in keyhole plasma arc welding [J]. Trans Nonferrous Met Soc China, 2004, 14(1): 116−120.

[11] WANG Hui-jun. Close-loop control of welding stability based on image sensing during variable polarity plasma arc welding [D]. Harbin: Harbin Institute of Technology, 1998. (in Chinese)

[12] DONG Chun-lin, ZHU Yi-feng, ZHANG Hui, SHAO Yi-chen, WU Lin. Study on front side arc light sensing in keyhole plasma arc welding [J]. Chinese Journal of Mechanical Engineering, 2001, 37(3): 30−33. (in Chinese)

[13] CHAI Guo-ming, ZHU Yi-feng. Mechanism and simple current model of plasma cloud in plasma arc welding [J]. Chinese Journal of Mechanical Engineering, 2006, 42(1): 178−186. (in Chinese)

[14] WANG Hai-yan, CHEN Qiang, SUN Zhen-guo, WANG Yao-wen, SUN Jiu-wen. Detection of keyhole size by arc signal processing [J]. Transactions of the China Welding Institution, 2000, 21(3): 24−26. (in Chinese)

[15] STEFFENS H D, KAYSER H. Automatic control for plasma arc welding with constant keyhole diameter [J]. Welding Journal, 1972, 51(06): 408−418.

[16] ZHANG S B, ZHANG Y M. Efflux plasma charge-based sensing and control of joint penetration during keyhole plasma arc welding [J]. Welding Journal, 2001, 80(7): 157−162.

[17] DONG Chun-lin, WU Lin, ZHU Yi-feng, ZHANG Hui, SHAO Yi-chen. Detection of efflux plasma voltage in keyhole plasma arc welding [J]. Aeronautical Manufacturing Technology, 1999(5): 60−62. (in Chinese)

(Edited by YANG Hua)